Molecular dynamics study of the melting of a supported 887-atom Pd decahedron

2009 J. Phys.: Condens. Matter 21 144204

(http://iopscience.iop.org/0953-8984/21/14/144204)

J. Phys.: Condens. Matter **21** (2009) 144204 (6pp) doi:10.1088/0953-8984/21/14/144204

Molecular dynamics study of the melting of a supported 887-atom Pd decahedron

D Schebarchov[1], S C Hendy[1,2] and W Polak[3]

[1] School of Chemical and Physical Sciences, Victoria University of Wellington, Wellington 6140, New Zealand
[2] MacDiarmid Institute for Advanced Materials and Nanotechnology, Industrial Research Ltd, Lower Hutt 5040, New Zealand
[3] Department of Applied Physics, Institute of Physics, Lublin University of Technology, ul. Nadbystrzycka 38, 20-618 Lublin, Poland

E-mail: dimaslave@yahoo.com

Received 14 July 2008, in final form 22 October 2008
Published 18 March 2009
Online at stacks.iop.org/JPhysCM/21/144204

Abstract

We employ classical molecular dynamics simulations to investigate the melting behaviour of a decahedral Pd_{887} cluster on a single layer of graphite (graphene). The interaction between Pd atoms is modelled with an embedded-atom potential, while the adhesion of Pd atoms to the substrate is approximated with a Lennard-Jones potential. We find that the decahedral structure persists at temperatures close to the melting point, but that just below the melting transition, the cluster accommodates to the substrate by means of complete melting and then recrystallization into an fcc structure. These structural changes are in qualitative agreement with recently proposed models, and they verify the existence of an energy barrier preventing softly deposited clusters from 'wetting' the substrate at temperatures below the melting point.

(Some figures in this article are in colour only in the electronic version)

1. Introduction

Theory and experiment have shown that the structure and physical properties of metal nanoparticles are strongly dependent on particle size [1]. In clusters of more than 100 atoms, corresponding to what is often referred to as the scaling regime, the dependence of physical properties upon size is relatively smooth, and it arises due to the changing surface to volume ratio. Because of significant surface and interfacial effects, metals that form a face-centred cubic (fcc) lattice in the bulk tend to form non-crystalline structures such as decahedra [2] and icosahedra [3] at the nanometre scale. These variations in structure, together with particle size, can result in intriguing and extremely useful thermodynamic, electronic and catalytic properties. These properties have already found use in a wide range of applications such as catalysis [4], gas sensing [5], hydrogen storage [6] and fabrication of various nanodevices.

However, most experiments with nanoparticles are carried out on a substrate, which may alter the crystal structure from that of the free cluster. The effects of lattice mismatch, deposition speed and particle size on the cluster–substrate epitaxy have all been studied extensively with computer simulations [7–9] and experiments [10–12]. Molecular dynamics (MD) simulations have shown that in both homoepitaxial and heteroepitaxial systems, there is an energy barrier hindering the deposited solid nanoclusters from accommodating themselves to the substrate [7]. MD simulations by Shintani *et al* [8] have demonstrated that clusters very close to their melting point accommodate themselves in a smooth fashion, similar to completely molten particles that experience no energy barrier at all. Järvi *et al* [9] have also employed MD simulations to study the homoepitaxy of Cu, Ag, Au, Pt and Ni clusters on (100) surfaces. These simulations were carried out at temperatures up to 750 K, showing gradual epitaxial alignment via a dislocation glide mechanism.

For some applications it may be desirable to preserve the structure of free clusters during and after their deposition on a substrate. This can be achieved by minimizing the impact energy upon deposition (i.e. soft landing [13]), working at lower temperatures and/or choosing a weakly interacting supporting surface. If the cluster sustains no mechanical damage during the landing, its morphological evolution will

be strongly dependent on the temperature and the interaction with the substrate.

The effects of cluster–substrate interactions on the melting of nanoparticles have previously been studied by Ding *et al* [14]. Their MD simulations of Fe clusters supported on an 'ideal', unstructured substrate have shown that melting is initiated at the free surface, whereas the mobility of metal atoms that are in contact with the static and perfectly smooth substrate is retarded due to pinning. They found a relatively simple dependence of the melting temperature T_{m} on the size of the supported nanocluster: $T_{\mathrm{m}} \propto R_{\mathrm{eff}}^{-1}$, where R_{eff} refers to the 'effective radius', or simply the radius of curvature of the supported nanoparticle when relaxed. One of the implications of this result is that a free nanocluster will have a lower melting temperature than a supported cluster of equal volume, despite the fact that the supported cluster will generally have a higher surface to volume ratio. However, epitaxial strains at the cluster–substrate interface are neglected in Ding *et al*'s simulations. Hendy [15] has considered the possible effects of epitaxial strain and shown that the model of Ding *et al* should only hold in the special case where the radii of curvature of the relaxed solid and liquid phase particles are identical. If the curvature of the solid and liquid particles differ due to epitaxial strains, then the melting temperature will not follow this simple dependence on size.

In this paper, we investigate the thermal stability of a particular nanocrystalline palladium structure after a soft landing on a single layer of graphite. We then qualitatively compare our simulation results with the predictions of the current thermodynamic models. In our simulations we focus on a closed-shell 887-atom Marks decahedron, which is shown to be energetically and thermodynamically stable as a free cluster at this size. Palladium nanostructures are often used in catalysis [16] and gas sensing [5], and their performance is strongly dependent on crystal structure. We chose graphite as our substrate because it is known to interact very weakly with most pure metals [17], making it ideal for the purpose of retaining the initial structure of deposited metal nanoclusters.

2. Computational details

The simulated system comprised a closed-shell Pd_{887} Marks decahedron resting on a single layer of graphite (87.6 Å by 88.5 Å). Since we are interested in softly deposited clusters with no sustained damage upon impact, the initial configurations were generated by simply *placing* the cluster near the supporting surface (the closest Pd atom is within two bond lengths of the substrate). The generated geometries were then equilibrated at 1000 K for 125 ps. Simulations were carried out on a static graphene sheet, where the constituent carbon atoms were fixed in a honeycomb lattice with a nearest-neighbour separation of 1.46 Å. All of the palladium atoms were simulated in the canonical (NVT) ensemble by coupling them to the Langevin thermostat [18]. The friction parameter γ in the Langevin equation of motion was chosen by trial and error ($\gamma_{\mathrm{Pd}} = 9.45\ \mathrm{ps}^{-1}$) to ensure adequate conservation of temperature and quick equilibration. The equations of motion were integrated using the Velocity–Verlet algorithm with a timestep of 2.5 fs.

The interactions between Pd atoms in the metal cluster were modelled with an embedded-atom (EAM) potential parametrized by Zhou *et al* [19], which is truncated at 6 Å. To our knowledge, this potential has not yet been used to study the melting of palladium, hence we tested its adequacy by calculating the melting temperature ($T_{\mathrm{m}}^{\mathrm{bulk}}$) of bulk Pd at zero pressure. We estimate that $T_{\mathrm{m}}^{\mathrm{bulk}} \approx 1630$ K, which is lower than the experimentally obtained value of 1828 K, but of comparable merit to other EAM potentials [20]. However, most critical to this study is the adhesion of the Pd cluster to the substrate. The Lennard-Jones (LJ) potential provides an adequate description of the weak Pd–C interaction, and it has been used previously for this purpose [21]. LJ parameters for the Pd–C interaction were taken directly from [21]: $\epsilon = 33.5$ meV and $\sigma = 2.926$ Å. The long attractive tail of this pair potential was smoothly truncated at 3.2σ.

Caloric curves were calculated using two different procedures. First, we gradually heated the cluster from 1000 to 1500 K in steps of 10 K and equilibrated at each temperature for 0.5 ns. After equilibration, average quantities were collected over a further 0.5 ns. The second procedure comprised a collection of completely independent NVT simulations around the melting transition, where at each temperature the equilibration lasted 2.5 ns and the production stage ran for 1.25 ns.

Two different methods were used to analyse the structural evolution of the supported cluster. First, we followed Cleveland *et al* [22] in using the bimodality of the distribution of diffusion coefficients to distinguish less mobile, solid-like atoms from the highly diffusive, liquid-like atoms. Second, the cluster's internal structure was also analysed and visualized using the structural analysis scheme of Polak [23], which is based on the coordination polyhedron (CP) method [24]. In this latter method, atoms with a complete first coordination shell (composed of 12 first neighbours) are found, and the local structure around every fully coordinated atom is classified by recognizing the shapes of coordination polyhedra. These polyhedra allow identification of face-centred cubic (fcc), hexagonal close-packed (hcp), icosahedral (ic) and decahedral (dh) local structures. Even though this method fails to account for the structure of atoms without a complete first coordination shell (e.g. surface atoms), it is a fast and reliable alternative to the common neighbour analysis (CNA) [25] scheme.

3. Results and discussion

Considering the weak nature of the cluster–substrate interaction employed in this study, one would expect stable nanocrystalline structures to remain stable, or at least metastable, after a controlled landing on the substrate. Presumably, sufficiently weak cluster–substrate interactions should in no way alter the crystal structure or the melting behaviour of supported clusters. However, in the regime where a softly deposited nanocrystalline structure is only metastable, one can expect interesting

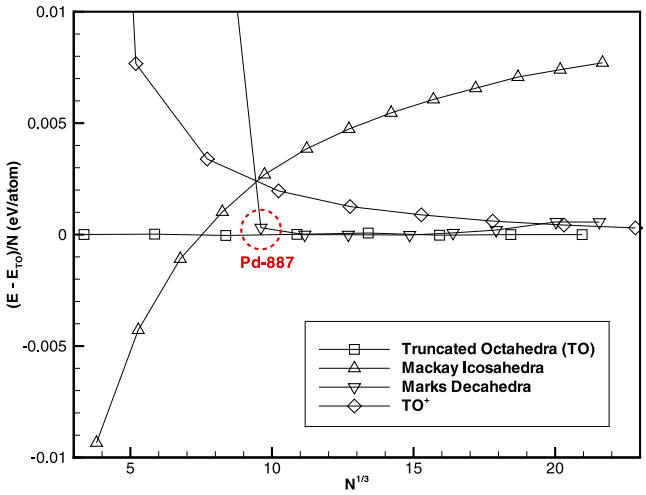

Figure 1. Comparison of the relaxed zero temperature binding energies of various closed-shell structures (represented by symbols) of Pd nanoclusters. Icosahedral clusters have the lowest binding energy for $N \leqslant 309$, whereas for $887 \leqslant N \leqslant 4405$ there is a strong competition between Marks decahedra and truncated cubo-octahedra. At large cluster sizes, crystalline fcc structures (TO and TO$^+$) become most energetically favourable.

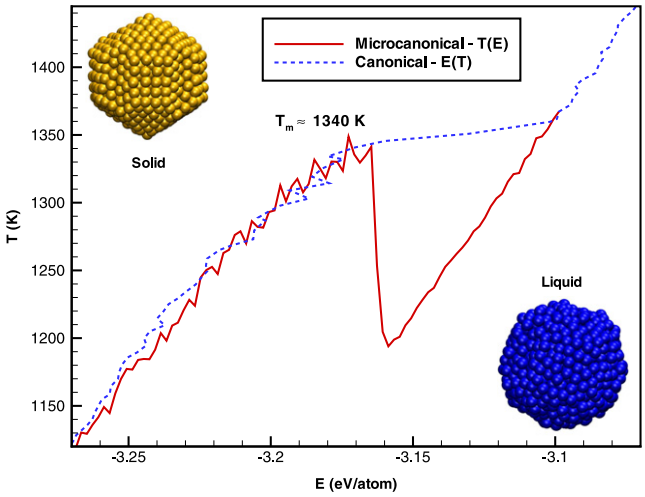

Figure 2. Caloric curves of the melting transition in a free Pd_{887} Marks decahedron. The two curves show that melting occurs at 1340 K (-3.165 eV/atom), and neither of them exhibits any unusual behaviour prior to or during the phase transition.

behaviour at elevated temperatures, particularly near the melting transition. The following series of findings gives a good example of the novel melting behaviour of metastable structures on a substrate.

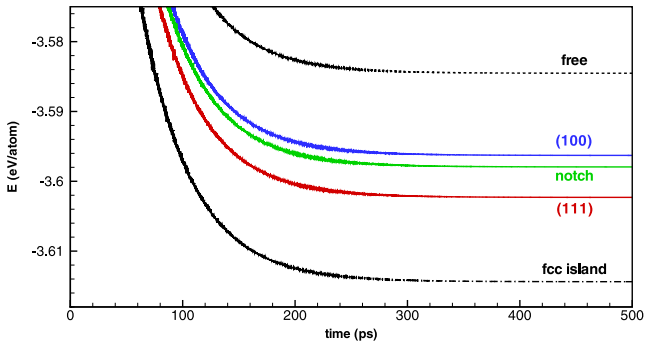

Figure 4. Solid lines represent the evolution of the total potential energy of the supported Pd_{887} decahedron, resting on different facets, during the simulated annealing. The dash-dotted curve corresponds to the annealing of a frozen 887-atom nanodroplet, whereas the energy of the free Pd_{887} is given by the dashed line.

3.1. Stability of free Pd_{887}

Prior to introducing the substrate effects, we first look at the energetic and thermal stability of a free Pd_{887} Marks decahedron. This will later allow us to elucidate the substrate effects by direct comparison with the energetics and thermodynamics of a supported Pd_{887}. Figure 1 shows the calculated binding energies per atom for a series of closed-shell Pd structures. The binding energy of the 887-atom decahedron is relatively close to that of Pd_{586} and Pd_{1289}, both of which have a truncated cubo-octahedral structure. To verify the thermodynamic stability of the decahedral structure, we calculated its caloric curves in the canonical and microcanonical ensembles (see figure 2). Neither curve displays any solid–solid transitions or any other unusual behaviour prior to the melting point, indicating good thermodynamic and energetic stability of the Pd_{887} Marks decahedron under the EAM potential used in this study.

3.2. Thermal instability in supported Pd_{887}

A controlled deposition of a free Pd_{887} Marks decahedron can result in one of the three possible configurations: the cluster resting on either a (111) or (100) facet, or one of its notches (re-entrant facets). These three orientations are depicted in figure 3. The total potential energy of each geometry was calculated by means of equilibrating the system at 600 K, followed by an anneal to 0 K. Figure 4 shows the total energy associated with each cluster orientation during the simulated annealing. Since the cluster resting on one of its (111) facets yields the lowest potential energy, we shall focus our attention on this particular geometry.

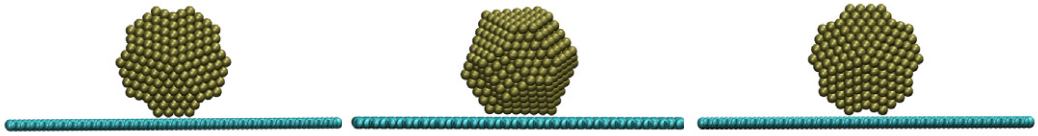

Figure 3. Three possible metastable orientations of the supported Pd_{887}: the cluster resting on either the (100) facet (left), the (111) facet (centre), or one of the re-entrant facets (right).

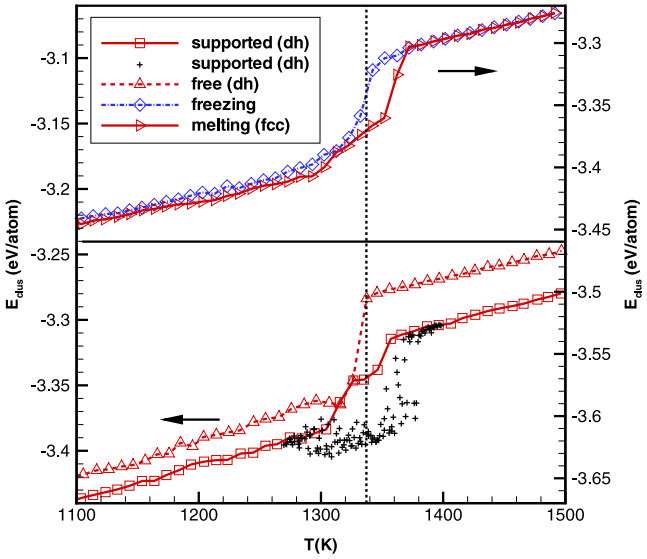

Figure 5. The bottom panel shows the variation in potential energy of the free (dashed line) and supported (solid line) Pd_{887} Marks decahedron during heating. The '+' symbols represent the independent canonical simulations of the supported decahedron. The top panel shows the variation in the potential energy of the supported Pd_{887} liquid droplet during cooling, and the supported Pd_{887} fcc island during heating. The vertical dashed line marks the melting point of the free Pd_{887} Marks decahedron, and the two black arrows point to the relevant energy axis.

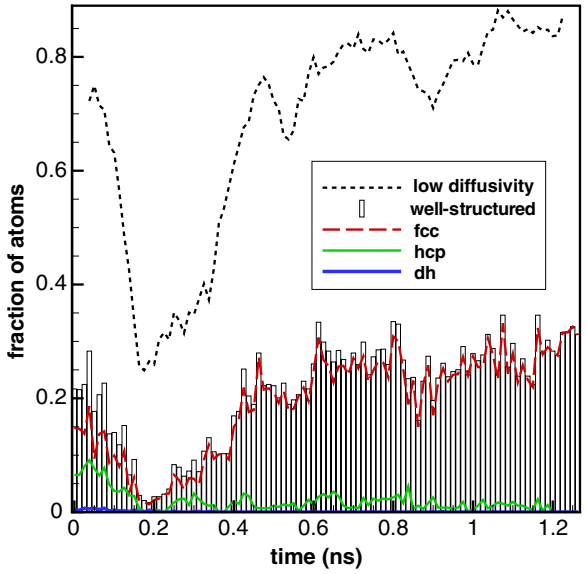

Figure 6. Structural evolution of the softly deposited Pd_{887} decahedron after equilibration at 1320 K. Initially, there is a significant fraction of fcc and hcp atoms, as well as some dh structure. At $t \approx 0.2$ ns complete loss of structure takes place, followed by gradual recrystallization into an fcc lattice. The top dashed line traces out the fraction of atoms with low diffusivity, which can be interpreted as 'solid'. The bars represent the fraction of atoms exhibiting good local order. The total fraction of well-structured atoms is defined as $N_{\mathrm{ord}} = (N_{\mathrm{fcc}} + N_{\mathrm{hcp}} + N_{\mathrm{dh}})/N$, where $N = 887$.

The thermal stability of the supported Pd_{887} Marks decahedron, with one of its (111) facets in contact with the graphene, was then tested by heating it from 1000 up to 1500 K. This conformation remains stable at temperatures up to 1150 K, above which diffusion of Pd atoms at the (100) and the re-entrant facets begins to occur. However, the five-fold twin planes and the interior of the cluster remain intact up to 1300 K. Figure 5 shows the variation in the internal potential energy of the particle during the heating process, and it can be seen that complete melting of the supported cluster happens at $T \approx 1360$ K. However, the phase transition is not as abrupt as in the free Pd_{887}, yielding a range of temperatures over which the 'melting' takes place. To ensure this is not an artefact of insufficient equilibration, a series of independent NVT simulations were carried out for $1275\ \mathrm{K} < T < 1400\ \mathrm{K}$. The resultant variation of the cluster's potential energy with temperature is also plotted in figure 5, and it shows significant fluctuations prior to and during the melting transition.

In order to elucidate the origin of these fluctuations, we now inspect the structural evolution of the supported cluster at 1320 K. Structural analysis of this particular simulation is shown in figures 6 and 7. From them we can see that, after an equilibration period of 2.5 ns, the nanoparticle is still decahedral at the beginning of the production run. Figure 6 traces the fraction of constituent fcc, hcp and dh atoms during the production run, as well as the fraction of atoms with low diffusion coefficients. There is a very good correlation between fluctuations in atom mobility and the degree of local structure, and both analysis methods indicate that almost complete melting of the cluster occurs at $t \approx 0.2$ ns. Prior to melting ($t < 0.2$ ns), the majority of interior atoms form an fcc lattice, but there is a significant fraction of hcp and a few dh atoms present. Figure 7 gives a visual description of the solid–solid transition, and it shows a well-defined five-fold twin boundary (hcp and dh atoms) still present in the early stage of the simulation. However, at $t \approx 0.2$ ns the cluster loses its crystallinity and remains disordered for a brief period of time, after which it takes on an fcc morphology with a vanishing hcp fraction. Figure 7(f) illustrates the crystal structure in the early stages of solidification, which appears to be initiated at the cluster–substrate interface. We also note that once some fcc structure is formed, it is always present adjacent to the cluster–substrate interface, whereas the local order of the rest of the cluster fluctuates.

Similar solid–solid transformations have been previously reported in microcanonical simulations of free Pt and Pd nanoclusters [26, 27]. These studies show that even though some nanocrystallites are stable at lower temperature, they can still undergo solid–solid transitions prior to or during solid–liquid phase coexistence, or via complete melting. Note that in this current study we do not observe such transformations in the free Pd_{887} Marks decahedron (see figure 2), indicating that the solid–solid transition seen in the graphene-supported cluster is most likely to be driven by substrate effects.

3.3. Role of substrate effects

Due to the weak nature of the cluster–substrate interaction in our simulations, we do not observe epitaxial alignment of

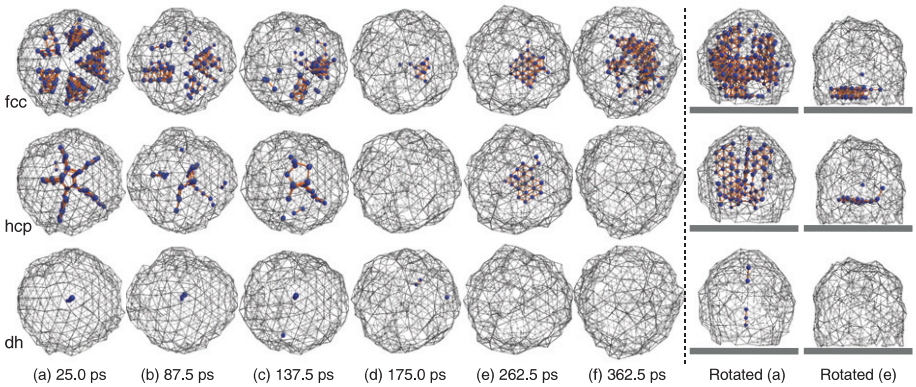

Figure 7. Visualization of the structural evolution of the cluster in the early stages of the production run at $T = 1320$ K. The snapshots illustrate the destruction of the five-fold twin boundary during melting (175.0 ps), followed by the early stages of recrystallization into an fcc lattice. The cluster is viewed along the five-fold symmetry line (represented by dh units in (a)–(c)), which is inclined to the substrate by an angle of 60°. Snapshots (a) and (e) have been rotated to give a more precise illustration of the initial structure, and to point out that recrystallization is initiated at the graphite monolayer (shown as grey rectangle).

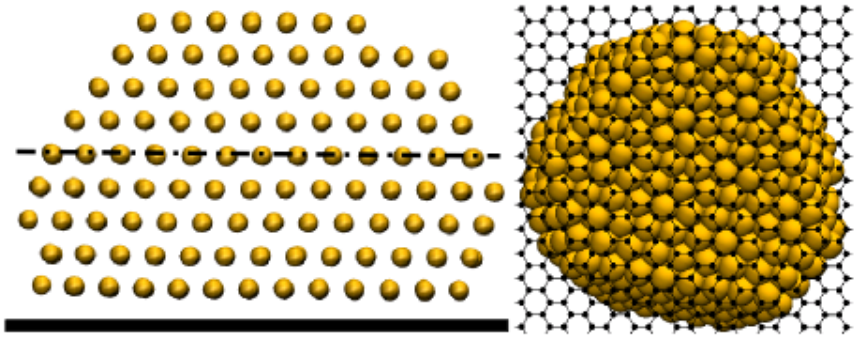

Figure 8. Frozen Pd_{887} nanodroplet annealed to zero temperature. Snapshot on the left is take from the side, viewing parallel to the substrate (narrow black rectangle underneath). The horizontal dash-dot line marks the location of the twin boundary. Snapshot on the right is taken from below the frozen fcc island, viewing perpendicular to and through the graphite layer.

Pd atoms with the fixed C atoms in the substrate. The Pd–C interactions are insufficient to initiate the dislocation glide mechanism [9], hence the internal structure of the deposited Marks decahedron is retained while it is still solid. However, when the decahedron melts, liquid atoms in the bottom layer get pinned to the substrate, initiating the formation of a Pd(111) facet at the cluster–substrate interface (see figure 8). The size and structure of this facet dictate the consequent recrystallization into an fcc structure.

The total energy of a Pd_{887} nanodroplet frozen on graphene is significantly lower than that of a supported Pd_{887} Marks decahedron at zero temperature (see figure 4), verifying that the graphene-supported decahedron is only metastable at low temperatures. However, a molten nanodroplet spontaneously wets the substrate and quickly finds the globally stable conformation. Gradually freezing the molten cluster and annealing it to zero temperature leads to the formation of an fcc island, whose structure is shown in figure 8. The frozen island has a single twin boundary formed parallel (but not adjacent) to the substrate, but the rest of the atoms form a regular fcc lattice. The atomic layer in contact with the graphene sheet is a defect-free (111) facet, which is a close-packed facet and hence maximizes the Pd–C interaction. The caloric curve associated with the freezing process is also shown in figure 5.

Failure of the solid Pd_{887} to spontaneously 'wet' the substrate indicates the presence of a significant energy barrier [7, 8]. Presumably, the barrier is highest for closed-shell structures that sustain no damage during the deposition, nor cause any significant damage to the substrate.

At the instant when the decahedral structure melts, the system consists of an almost spherical droplet adjacent to the graphene layer. The liquid cluster spontaneously spreads along the substrate, forming a spherical cap, and finds the energetically favourable geometry without experiencing any significant energy barriers [8]. Even though the resultant conformation increases the total surface area of the cluster, it leads to stabilization of the surface atoms and hence, minimization of the surface energy. In effect, the stabilization and pinning of atoms at the interfaces increases the melting temperature of the cluster, which leads to recrystallization into an fcc structure. This apparent rise of the melting temperature after an increase in the 'effective radius' of the supported droplet is consistent with the models proposed by Ding *et al* [14] and Hendy [15]. Figure 5 shows that a supported Pd_{887} cluster undergoes complete melting roughly 20 K above the melting temperature of a free Pd_{887} Marks decahedron. We expect that a stronger cluster–substrate interaction will yield an even higher increase in the melting temperature.

4. Summary

We have performed MD simulations of an 887-atom Pd Marks decahedron supported on graphene. Our simulations suggest that a free Pd_{887} decahedron is thermodynamically stable prior to melting, whereas the structure becomes metastable once deposited on graphene. The supported Marks decahedron remains trapped in the metastable state at temperatures up to 1300 K, which is only 60 K below the complete melting point. For 1300 K $< T <$ 1360 K, we find the cluster accommodates to the substrate by melting, then wetting the substrate, followed by recrystallization into an fcc structure. The observed solid–solid transition provides new evidence that such transformations could occur in real experiments involving metal nanoparticles on substrates. The mechanism driving this transformation is different from that of free particles and is attributed primarily to substrate effects. We also find that the double melting transition of the graphene-supported Pd_{887} is in qualitative agreement with the recently proposed thermodynamic models [14, 15].

References

[1] Baletto F and Ferrando R 2005 Structural properties of nanoclusters: energetic, thermodynamic, and kinetic effects *Rev. Mod. Phys.* **77** 371

[2] Marks L D 1984 Surface structure and energetics of multiply twinned particles *Phil. Mag.* A **49** 81

[3] Ino S and Ogawa S 1967 Multiply twinned particles at earlier stages of gold film formation on alkalihalide crystals *J. Phys. Soc. Japan* **22** 1365

[4] Hamilton J F and Baetzold R C 1979 Catalysis by small metal clusters *Science* **205** 1213

[5] van Lith J, Lassesson A, Brown S A, Schulze M, Partridge J G and Ayesh A 2007 A hydrogen sensor based on tunneling between palladium clusters *Appl. Phys. Lett.* **91** 181910

[6] Campesi R, Cuevas F, Gadiou R, Leroy E, Hirscher M, Vix-Guterl C and Latroche M 2008 Hydrogen storage properties of Pd nanoparticle/carbon template composites *Carbon* **46** 206

[7] Lei H L, Hou Q and Hou M 2000 Effect of cluster size on Cu/Au (111) epitaxy *J. Phys.: Condens. Matter* **12** 8387

[8] Shintani K, Taniguchi Y and Kameoka S 2004 Molecular-dynamics analysis of morphological evolution of softly deposited Au nanoclusters *J. Appl. Phys.* **95** 8207

[9] Järvi T T, Kuronen A, Meinander K, Nordlund K and Albe K 2007 Contact epitaxy by deposition of Cu, Ag, Au, Pt, and Ni nanoclusters on (100) surfaces: size limits and mechanisms *Phys. Rev.* B **75** 115422

[10] Bromann K, Brune H, Flix C, Harbich W, Monot R, Buttet J and Kern K 1997 Hard and soft landing of mass selected Ag clusters on Pt(111) *Surf. Sci.* **377–379** 1051

[11] Li B Q and Zuo J M 2005 Structure and shape transformation from multiply twinned particles to epitaxial nanocrystals: importance of interface on the structure of Ag nanoparticles *Phys. Rev.* B **72** 085434

[12] Sato K, Huang W J, Bohra F, Sivaramakrishnan S, Tedjasaputra A P and Zuo J M 2007 Size-dependent structural transition from multiple-twinned particles to epitaxial fcc nanocrystals and nanocrystal decay *Phys. Rev.* B **76** 144113

[13] Cheng H and Landman U 1994 Controlled deposition and classification of copper nanoclusters *J. Phys. Chem.* **98** 3527

[14] Ding F, Rosén A, Curtarolo S and Bolton K 2006 Modeling the melting of supported clusters *Appl. Phys. Lett.* **88** 133110

[15] Hendy S C 2007 A thermodynamic model for the melting of supported metal nanoparticles *Nanotechnology* **18** 175703

[16] Hwang C-B, Fu Y-S, Lu Y-L, Jang S-W, Chou P-T, Wang C R C and Yu S J 2000 Synthesis, characterization, and highly efficient catalytic reactivity of suspended palladium nanoparticles *J. Catal.* **195** 336

[17] Lee J, Tanaka T, Seo K, Hirai N, Lee J-G and Mori H 2006 Wetting of Au and Ag particles on monocrystalline graphite substrates *Rare Metals* **25** 469

[18] Adelman S A and Doll J D 1976 Generalized Langevin equation approach for atom/solid-surface scattering: general formulation for classical scattering off harmonic solids *J. Chem. Phys.* **64** 2375

[19] Zhou X W, Johnson R A and Wadley H N G 2004 Misfit-energy-increasing dislocations in vapor-deposited CoFe/NiFe multilayers *Phys. Rev.* B **69** 144113

[20] Jeong J-W and Chang K J 1999 Molecular-dynamics simulations for the shock Hugoniot meltings of Cu, Pd and Pt *J. Phys.: Condens. Matter* **11** 3799

[21] Sankaranarayanan S K R S, Bhethanabotla V R and Joseph B 2005 Molecular dynamics simulations of the structural and dynamic properties of graphite-supported bimetallic transition metal clusters *Phys. Rev.* B **72** 195405

[22] Cleveland C L, Landman U and Luedtke W D 1994 Phase coexistence in clusters *J. Phys. Chem.* **98** 6272

[23] Polak W 2006 Size dependence of freezing temperature and structure instability in simulated Lennard-Jones clusters *Eur. Phys. J.* D **40** 231

[24] Polak W and Patrykiejew A 2003 Local structures in medium-sized Lennard-Jones clusters: Monte Carlo simulations *Phys. Rev.* B **67** 115402

[25] Clarke A S and Jónsson H 1993 Structural changes accompanying densification of random hard-sphere packings *Phys. Rev.* E **47** 3975

[26] Schebarchov D and Hendy S C 2007 Thermal instability of decahedral structures in platinum nanoparticles *Eur. Phys. J.* D **43** 11

[27] Schebarchov D and Hendy S C 2006 Solid–liquid phase coexistence and structural transitions in palladium clusters *Phys. Rev.* B **73** 121402